THE JOURNAL OF PHYSICAL CHEMISTRY B

Article

pubs.acs.org/JPCB

Adenosine-Triggered Elimination of Methylene Blue Noncovalently Bound to Immobilized Functional dsDNA-Aptamer Constructs

Yun Dai, Banani Chakraborty, Bixia Ge, and Hua-Zhong Yu*

Department of Chemistry, Simon Fraser University, Burnaby, British Columbia V5A 1S6, Canada

Supporting Information

ABSTRACT: Immobilization and electrochemical characterization of specially designed functional DNA−aptamer constructs are of great importance for the development of versatile biosensors (not limited to gene analysis) and the investigation of molecular interactions between DNA and other molecules. We have constructed a "DNA conformational switch" by incorporating the antiadenosine aptamer sequence in the middle of an otherwise cDNA double helix, as its structural change responds to the presence of small molecule ligands (e.g., adenosine). In particular, methylene blue (MB) was used as a model system to probe the rather complex interaction modes between small redox molecules and the dsDNA−aptamer construct. Besides intercalating with the double-stranded DNA stem, MB can stack with a single guanine base in the relatively unstructured aptamer domain or electrostatically bind to the DNA backbone. The decreased surface density of MB after adenosine binding indicated that the ligand-gated structural change of the dsDNA−aptamer construct can eliminate MB molecules that were originally bound to the aptamer domain but not those in the complementary stem.

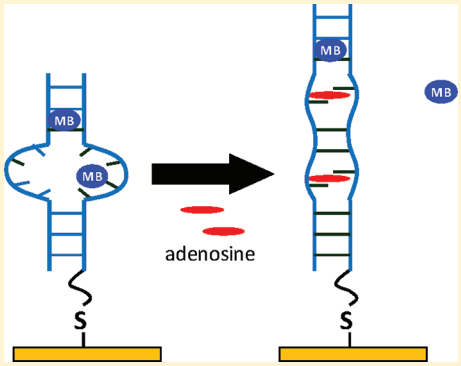

INTRODUCTION

Aptamers are molecular receptors typically made of single-stranded DNA or RNA.[1,2] They have specific, high binding affinities for a variety of targets including metal cations,[3] small organic molecules,[4] and proteins.[5] Compared with conventional antibodies, aptamers have the following advantages for biosensing applications.[6−13] First, aptamers are screened by the SELEX (systematic evolution of ligands by exponential enrichment) approach; this in vitro selection overcomes the limitation of using cell lines or animals that are necessary for producing antibodies. Second, the rather simple and robust chemical structure of single-stranded DNA makes it easy to modify aptamers with desired functional groups. Third, aptamers can function at harsh conditions, whereas antibodies require a physiological environment.[6] The original sequence for the antiadenosine DNA aptamer was selected in the 1990s and has been well characterized by NMR analysis.[4,14] It has been chosen as one of the model systems for the development of novel aptamer-based biosensors, based on a variety of electrochemical and optical signal readout methods.

Electrochemistry is one of the most popular signal transduction approaches for the development of portable biosensors.[15,16] Because nucleobases react irreversibly at extreme electrode potentials, it is necessary to introduce an "external" redox marker that can undergo reversible electrochemical processes. Methylene blue (MB), a phenothiazine dye, has been used as a redox marker for studying DNA-modified electrodes.[17] It is converted to leucomethylene blue (LB) by two-electron reduction with a formal potential in the range of −0.10 to −0.40 V (vs SCE) at pH 4−11.[18] Recently,[19] MB has been used as a redox label and covalently tethered to one terminal nucleobase of single-stranded DNA (containing the sequence of antithrombin aptamer) that immobilized on a gold electrode. As a result of the formation of a G-quadruplex upon binding thrombin, the distance between the bound MB and the gold electrode is increased, and a decrease of the peak current is observed.[19]

In the past, solution-diffused MB has also been used as a redox marker because it can bind DNA noncovalently.[20−34] First, positively charged MB in solution electrostatically binds to the negatively charged DNA phosphate backbones of ssDNA and dsDNA.[20,21] Second, spectroscopic and electrochemical results have shown that the aromatic planar structure of MB facilitates its intercalation with two successive DNA base pairs.[17,22−27] For example, the fluorescence polarization of MB increased after binding with dsDNA, whereas electrostatic or DNA groove binding would not result in such an enhancement.[27] Third, both theoretical and experimental studies have suggested that MB can directly "stack" with a single guanine base. By varying the number of guanine bases in a short ssDNA, Yang et al. found that MB can interact with guanine bases specifically.[28] The free energy change of the MB−guanine complex formation was calculated to be −7.2 ± 0.2 kcal/mol.[29] Therefore, MB has been considered as a promising redox marker to develop probe-label-free biosensors.[30−34]

Fahlman and Sen have designed so-called "DNA conformational switches" by incorporating an antiadenosine aptamer in

Received: March 29, 2012
Published: May 23, 2012

   dx.doi.org/10.1021/jp302988t | J. Phys. Chem. B 2012, 116, 6361−6368

the middle of an otherwise cDNA duplex.[35] On the basis of gel electrophoresis assays, they found that the adenosine-triggered conformational change in the apatmer domain facilitates charge transfer through this dsDNA–aptamer construct. In our work, by immobilizing such dsDNA–aptamer constructs on a gold electrode, we can directly evaluate its interaction with redox indicators before and after binding adenosine. Therefore, this study focuses on a better understanding of the binding nature between intercalative molecules (e.g., MB) and specially designed DNA constructs, which is beneficial to the future development of more sensitive and selective biosensing and switching devices.

EXPERIMENTAL SECTION

Materials and Reagents. All reagents were obtained in their highest available purity and used without further purification unless otherwise noted. Both HPLC-purified thiol-modified and unmodified DNA oligonucleotides were purchased from Biosearch Technologies, Inc. (Novato, CA). After reducing the disulfide bond of the modified ssDNA (strand 1), the activated strand 1 was hybridized with unmodified ssDNA (strand 2 or 3) to form the dsDNA–apatmer constructs (apt–DNA) or a fully cDNA duplex (dsDNA), respectively.

Gold substrates (100 nm Au/5 nm Cr/glass) were purchased from Evaporated Metal Films Inc. (Ithaca, NY) and hexaammineruthenium(III) chloride, $Ru(NH_3)_6Cl_3$ (98%), and methylene blue chloride from Sigma-Aldrich (Milwaukee, WI). Deionized water (>18.3 MΩ cm) from a Barnstead Easy Pure UV/UF compact water system (Dubuque, IA) was used in all experiments. All plasticware was presiliconized.

Preparation of the DNA Constructs in Solution and Gel Assay. For the biochemical test, the dsDNA–aptamer construct (i.e., the DNA construct that incorporates the antiadenosine aptamer, apt-DNA) and the cDNA duplex (dsDNA) were formed by annealing equimolar mixtures (2 μM each) of the constituent strands in the binding buffer (10 mM Tris-HCl, 150 mM LiCl, 3 mM $MgCl_2$, 0.1 mM EDTA, and pH 8.2), as shown in Figure 1. The mixture was heated to 80 °C for 5 min and then cooled slowly to room temperature; 12% nondenaturing gel was run to confirm the formation of the apt–DNA and dsDNA with and without adenosine by comparing the gel mobility with that of each ssDNA. A 19:1 acrylamide/bisacrylamide solution was used as stock solution. The loading volume of each individual lane was 10 μL. The gels were run in a SE600 Series Standard Vertical Electrophoresis Unit at 300 V for 1.5 h. Bromophenol Blue and Xylene Cyanol FF were gel loading dye to track the positions of the DNA strands on the gel. After running, the gels were stained with "stains all" solution for 2 h and destained before scanning.

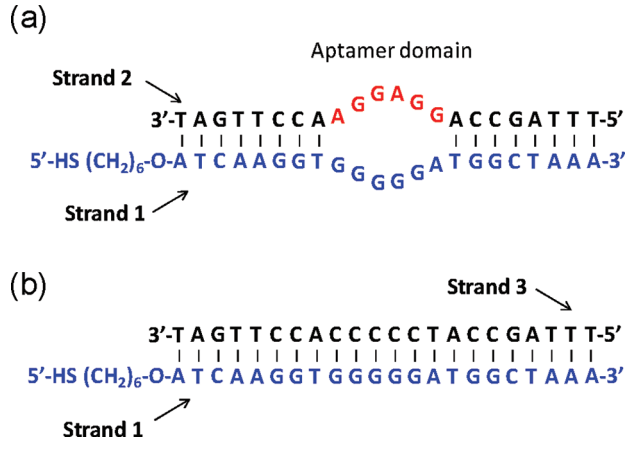

Figure 1. Illustration of secondary structure of (a) the dsDNA–aptamer construct (apt–DNA) and (b) the complementry DNA duplex (dsDNA).

Preparation of DNA-Modified Electrodes. A 4 h incubation of the thiol-modified ssDNA (strand 1) with 10 mM tris(2-carboxyethyl)phosphine hydrochloride (TCEP, Aldrich-Sigma) in the binding buffer was necessary to activate this ssDNA by reducing the disulfide bond. By varying the initial amount of strand 1, we were able to control the surface density of dsDNA on the gold electrode. A MicroSpin G-50 column, rinsed with deoxygenated binding buffer prior to use, was applied to filter potential impurities. Then, the concentration of the purified strand 1 was measured with a Nanodrop ND-1000 spectrophotometer (Davis, CA). Equal amounts of strand 2 or 3 were added to strand 1, followed by annealing to form apt–DNA and dsDNA, respectively. Prior to modification, the gold chips were cleaned with freshly prepared piranha solution [3:1 (v/v) mixture of concentrated H_2SO_4 and 30% H_2O_2 (WARNING: piranha solution reacts violently with organic solvents and must be handled with extreme care)] at 90 °C for 5 min and then rinsed thoroughly with deionized water. A 20 μL droplet of apt–DNA or dsDNA was then immediately spread on the surface of the gold chip, and the DNA-coated chips were stored in a box at 100% relative humidity and room temperature for 15–30 h. After DNA immobilization, 1 h incubation of 1 mM 6-mercapto-1-hexanol (MCH) was applied to passivate the gold surface and remove nonspecifically adsorbed DNA. Finally, the gold chips were rinsed thoroughly with 10 mM Tris buffer (pH 8.2). Prior to the electrochemical measurements, all the modified gold chips were stored with binding buffer in a box with 100% relative humidity at room temperature.

Electrochemical Measurements. All electrochemical experiments were carried out using a 10 mL three-electrode cell with a DNA-modified gold chip as the working electrode (with a geometric area of 0.66 cm^2). An Ag|AgCl|3 M NaCl reference electrode and a Pt wire counter electrode were used. The CV measurements of both $[Ru(NH_3)_6]Cl_3$ and MB were performed at room temperature using an μAutolab II potentiostat/galvanostat (Eco Chemie B.V. Utrecht, The Netherlands) with different buffer systems: 10 mM Tris (10 mM Tris-HCl, pH 8.2) and binding buffer (10 mM Tris-HCl, 150 mM LiCl, 3 mM $MgCl_2$, 0.1 mM EDTA, pH 8.2) for $[Ru(NH_3)_6]Cl_3$ and MB, respectively. Usually, the cathodic peak of the first scan at 0.5 V/s of $[Ru(NH_3)_6]Cl_3$ was integrated to determine the DNA surface density on gold.[36,37] Prior to determining the MB surface density, the $[Ru(NH_3)_6]Cl_3$ in the cell was removed by gentle washing with Tris buffer followed by incubation with binding buffer for 20 min.[38] The cathodic peak of MB at 0.1 V/s after 30 min equilibration was used to determine the surface density of MB before and after adding adenosine. The incubation time of adenosine was fixed at 15 h. In the test of selectivity, the incubation times of AMP, GMP, UMP, and the blank were also 15 h. AMP and adenosine were removed by gently washing the electrode with binding buffer three to five times and incubating with binding buffer for at least 20 min. A stable CV after removing each target served as background for the following tests.

dx.doi.org/10.1021/jp302988t | J. Phys. Chem. B 2012, 116, 6361–6368

RESULTS AND DISCUSSION

Confirmation of the Formation of the dsDNA–Aptamer Construct. The formations of apt–DNA and dsDNA constructs were confirmed by nondenaturing gel electrophoresis (Figure 2). Either in the presence or in the absence of 1.0 mM adenosine, the lanes of the mixtures of ssDNA strands (1 + 2, or 1 + 3) after annealing showed only one band, respectively, with slower mobility than any ssDNA (Figure 2). This confirms that both apt–DNA (strands 1 + 2) and dsDNA (strands 1 + 3) can form under the specified experimental conditions and that adenosine does not cause dehybridization of these duplexes. In addition, it was shown that the three ssDNA strands have slightly different gel mobilities. Considering that strands 1 and 2 are guanine-rich, they potentially self-fold to certain tertiary structures that have faster gel mobility than strand 3 (which contains less guanine).[39] Although both strands 1 (in lane 1) and 2 (in lane 2) moved faster than strand 3 (in lane 3), the mixture of strands 1 and 2 (lanes 4 and 5: apt–DNA) moved slightly slower than the mixture of strands 1 and 3 (lanes 6 and 7: dsDNA). This indicated that the aptamer region affects the gel mobility of the DNA constructs, which further confirmed the formation of a stable DNA conformational switch (apt–DNA).

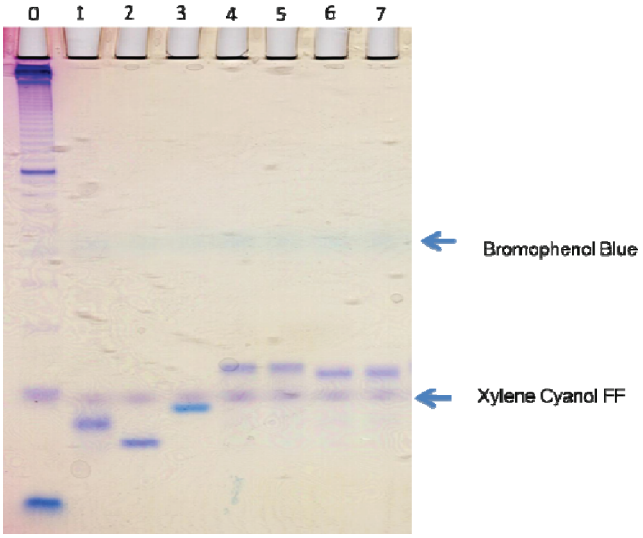

Figure 2. Gel electrophoresis analysis of the formation of DNA constructs: 14% nondenaturing polyacrylamide gel is run at room temperature at 300 V for 2.5 h. Lane 0: 10 base-pair ladder marker. Lane 1: strand 1 (thiolated DNA with 22 nucleotides). Lane 2: strand 2 (22 nucleotides forming apt–DNA with strand 1). Lane 3: strand 3 (22 nucleotides forming dsDNA with strand 1). Lane 4: apt–DNA formed by partial hybridization of strand 1 and 2. Lane 5: mixture of strands 1 and 2 incubated overnight with 1.0 mM adenosine. Lane 6: dsDNA formed by complete hybridization of strands 1 and 3 (22 base pairs). Lane 7: mixture of strands 1 and 3 incubated overnight with 1.0 mM adenosine.

Cyclic Voltammetry of Methylene Blue Noncovalently Bound to a DNA-Modified Gold Electrode. Figure 3a shows the CV curves of 5.0 μM methylene blue on an apt–DNA-modified gold electrode. When the electrode potential was scanned toward negative, MB was reduced to LB (leucomethylene blue) via a two-electron process and protonation. E_{pa} and E_{pc} were observed near −0.26 and −0.29 V (vs Ag/AgCl). More importantly, the linear relationship between the scan rate and the cathodic peak current shown in Figure 3b indicates that MB is bound to the DNA-modified surface. Comparison of the cathodic and anodic peaks reveals that the two peaks are not symmetric, as previously observed by others.[17,40] Their significant separation may be due to the fact that the reduced form, LB, has a different molecular structure, and it is no longer positively charged; the interaction between LB and DNA is not the same as that between MB and DNA.

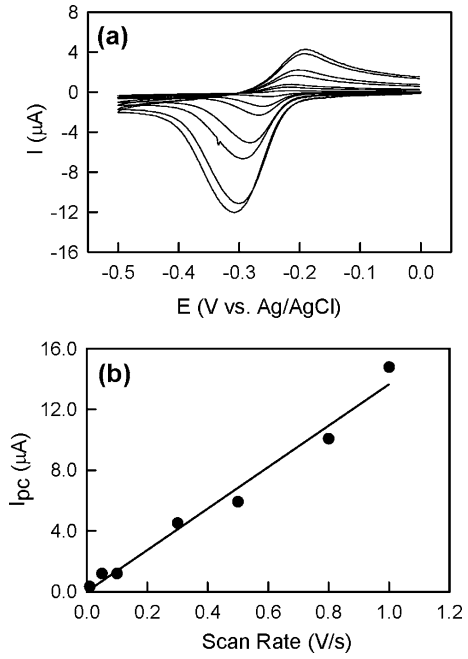

Figure 3. (a) Cyclic voltammetry of 5.0 μM methylene blue in 10 mM Tris-HCl, 150 mM LiCl, 3 mM $MgCl_2$, and 0.1 mM EDTA (pH 8.2) at an apt–DNA-modified gold electrode (area = 0.66 cm^2; scan rate = 10, 50, 100, 300, 500, 800, 1000 mV/s). (b) Plot of I_{pc} vs scan rate.

In another experiment, we also have investigated the time dependence of CV response upon adding MB. Figure 4 shows that the peak current increased sharply in the first 5 min, then gradually reached a plateau (within 30 min). Hence, a 30 min incubation period is required for quantitative analysis such as the adenosine binding study described in the following sections. Upon reaching equilibrium (e.g., after 30 min incubation), we carried out ten consecutive CV scans (without pause) and noticed that the MB peak current decreased dramatically after the first scan and then remained stable (data not shown). Subsequently, the peak current recovered in a new scan after only 15 s. A review of the binding mode between MB and DNA reveals that positively charged MB can associate with DNA via electrostatic interaction with the negatively charged phosphate backbone.[20,21] On the other hand, the reduced form, LB, is neutral; thus, after the first CV scan, LB may dissociate from the DNA, resulting in a decreased peak current. Non-electrostatically bound MB would remain on the DNA after several scans and generate a stable signal all the time. After the 15 s period of silence, MB in solution binds again electrostatically to the DNA, and the peak current recovers.

We also calculate the electron transfer rate constants of the DNA-surface-bound MB. As shown in Figure 3a, ΔE_p increased as a function of the scan rate, a phenomenon previously observed by Kelley et al.[17] They reported the cathodic potential of −0.25 V (vs SCE) for MB intercalating with dsDNA and the

dx.doi.org/10.1021/jp302988t | J. Phys. Chem. B 2012, 116, 6361–6368

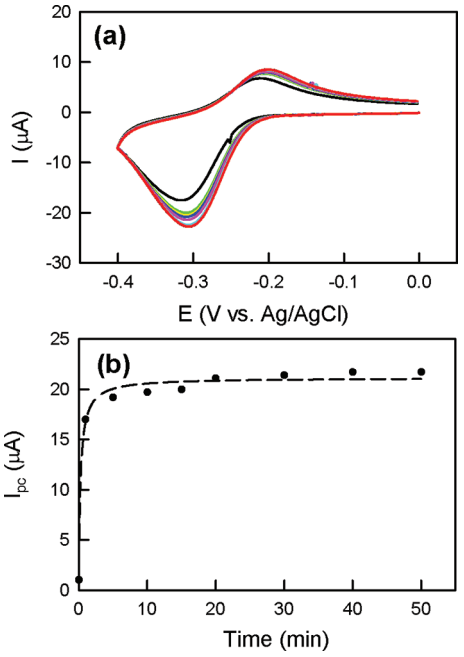

Figure 4. (a) Cyclic voltammetry of 5.0 μM methylene blue in 10 mM Tris-HCl, 150 mM LiCl, 3 mM $MgCl_2$, and 0.1 mM EDTA (pH 8.2) at an apt–DNA-modified gold electrode (area = 0.66 cm^2; scan rate = 1 V/s). The colored curve represents CV of MB with different incubation time (from black to red, the MB incubation time increased from 5 to 50 min). (b) Plot of I_{pc} vs incubation time of MB.

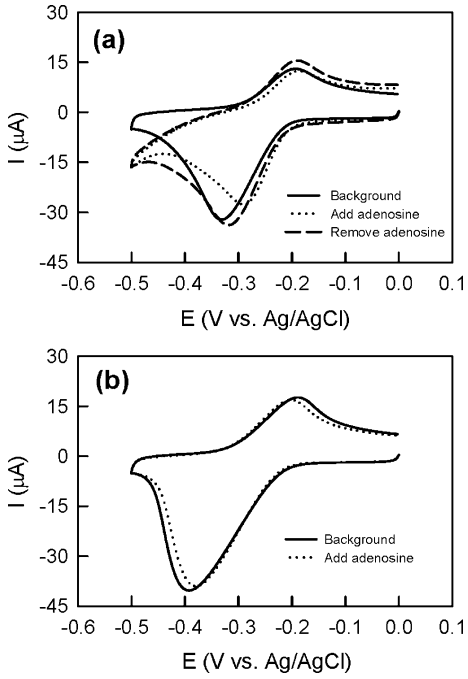

Figure 5. Electrochemical response of apt–DNA and dsDNA upon incubation with adenosine. (a) CV curves of 10 μM MB at an apt–DNA-modified gold electrode in 10 mM Tris-HCl, 150 mM LiCl, 3 mM $MgCl_2$, and 0.1 mM EDTA (pH 8.2) (electrode area = 0.66 cm^2; scan rate = 1 V/s). The solid line is the signal before adding adenosine, and the signal after adding adenosine is shown as a dotted line. The dashed line represents the signal after removing adenosine. (b) CV curves of 10 μM MB at a dsDNA-modified gold electrode in 10 mM Tris-HCl, 150 mM LiCl, 3 mM $MgCl_2$, and 0.1 mM EDTA (pH 8.2) (area = 0.66 cm^2; scan rate = 1 V/s). The solid line represents the signal before adding adenosine, and the signal after adding adenosine is shown as the dashed line.

increasing ΔE_p with faster scan rate. One possible reason is that the terminal aliphatic chain slows the electron transfer rate of the MB intercalating apt–DNA system.[41] On the basis of the Laviron theory,[42] the observed electron transfer rate constant k and the transfer coefficient α were found to be 3.8 ± 0.4 s^{-1} and 0.55 ± 0.02, respectively, i.e., much smaller than k = 1500 s^{-1} for MB adsorbed to mercury,[43] an indication that MB is located farther away from the electrode surface.

Adenosine-Induced Elimination of MB from the apt–DNA. The antiadenosine DNA aptamer was originally selected by Huizenga and Szostak.[4] Its structure has been well characterized by Lin and Petal.[14] It is interesting to examine the interaction modes between MB and apt–DNA change upon binding adenosine. As shown in Figure 5a, the peak current from MB decreased after introducing 1.0 mM adenosine to the apt–DNA-modified electrode and recovered after removal of the adenosine. In contrast, there is no signal change after adding adenosine to the dsDNA-modified electrode (Figure 5b). In their high-resolution NMR studies, Lin and Patel have confirmed that one DNA aptamer accommodates two AMP molecules by self-adaptive folding to a tight structure with facilitated base stacking.[14] Upon AMP binding, the "unstructured asymmetric internal loop" of the aptamer domain folds into two parallel triple-base platforms, widening the minor groove. Patel et al. summarized later that aptamers would usually show an induced-fit folding behavior upon target binding.[14,44] Therefore, initially we had expected that the adenosine binding induced formation of DNA triple-base platforms would allow more MB intercalated to the DNA construct. Accordingly, an increased peak current of MB should be observed upon incubation with adenosine. Considering the slight increase of the apparent electron transfer rate constant (4.6 ± 0.3 s^{-1}) upon adding adenosine, we believe that this surprising decrease in the peak current of MB is due to a conformational change of the aptamer domain. The most likely reason is that originally MB was stacked with a single guanine base in the aptamer domain;[28,29] upon adenosine-induced conformational change, this MB was eliminated and released into solution.

To estimate the number of MB molecules bound to either apt–DNA or dsDNA, we must determine the ratio of DNA duplex and MB surface densities. The surface density of the DNA-bound MB (Γ_{MB}) is obtained by integrating the reduction peak of the MB CVs (as shown in Figure 3) assuming that all surface-bound MB molecules are electroactive

$$\Gamma_{MB} = \frac{Q}{nFA} \quad (1)$$

where Q is the integrated charge of the cathodic peak; n is the number of electrons transferred; A is the electrode area; and F is the Faraday constant

The surface density of dsDNA can be readily measured by our previously reported protocol.[36,37] With 3.5 μM $Ru(NH_3)_6^{3+}$ added to the electrolyte, we can obtain reversible CVs of the $Ru(NH_3)_6^{3+}$ electrostatically bound to the DNA-modified electrodes.[36,37] The surface density of DNA constructs is then calculated by applying eqs 2 and 3

$$Q = nFA\Gamma_{Ru} \quad (2)$$

dx.doi.org/10.1021/jp302988t | J. Phys. Chem. B 2012, 116, 6361–6368

$$\Gamma_{DNA} = \Gamma_{Ru}\frac{Z}{m}N_A \quad (3)$$

where Z is the charge of the redox molecules ($Ru(NH_3)_6^{3+}$) and m is the number of nucleotides.

A typical CV of $Ru(NH_3)_6^{3+}$ on an apt−DNA-modified gold electrode is shown in Figure 6. Thus determined DNA surface

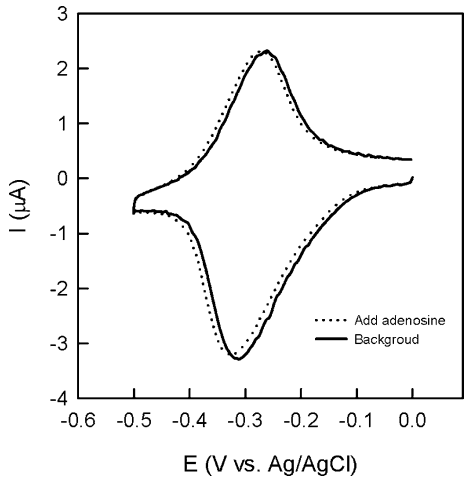

Figure 6. CV plots of 3.5 μM $Ru(NH_3)_6^{3+}$ in 10 mM Tris (pH = 8.2) at an apt−DNA-modified gold electrode (electrode area = 0.66 cm^2; scan rate = 100 mV/s) before and after binding adenosine. The surface density of apt−DNA can be determined from the integration of the reduction peak (see text for details).[36,37]

density did not change on addition of adenosine (the difference is within ±10%). This further confirms that the apt−DNA constructs are stable on the gold electrode when adenosine binds; i.e., no dehybridization or desorption takes place. We originally expected that a maximum of 7 MB molecules would bind to each dsDNA due to its rich GC base pair content.[45] The result is rather surprising: only one MB (0.98 ± 0.05) molecule was bound to each dsDNA, and the presence of adenosine in solution had no influence on this value. Kelley et al. obtained similar results[17] and proposed that a tightly packed dsDNA film on the surface restricts the access of solution-diffused MB to the potential binding sites. After the first MB binding, there is little chance for another MB to bind. Thus, we believe that only one MB molecule (average 0.98 ± 0.05) intercalates with GC pairs at the solution end of the dsDNA. In comparison, we found that at least two MB molecules were bound to apt−DNA (2.3 ± 0.2). Considering the structural differences between dsDNA and apt−DNA, the extra MB is probably binding to the guanine-rich aptamer domain. By immobilizing a series of synthetic ssDNA containing different numbers of guanine bases on a carbon paste electrode and making electrochemical measurements in MB solution, Yang et al. have shown that guanine bases in ssDNA have a specific affinity for MB. In particular, they found that the peak area of MB reduction increases with the number of guanine bases present in the ssDNA.[28] Moreover, a molecular dynamics simulation led Enescu et al. to propose a "stacking" conformation for the structure of guanine−MB complexes in water. The above findings support the likelihood that in apt−DNA the extra MB binds to the aptamer domain, as the guanine bases in this unstructured section behave like guanine bases in ssDNA.[29]

It should be noted that the above comparison holds for DNA films with the relatively low DNA surface density of 2×10^{11} to 7×10^{11} molecules/cm^2. At higher DNA surface densities, substantially smaller numbers of MB molecules were measured for both apt−DNA and dsDNA (Figure 7). More importantly,

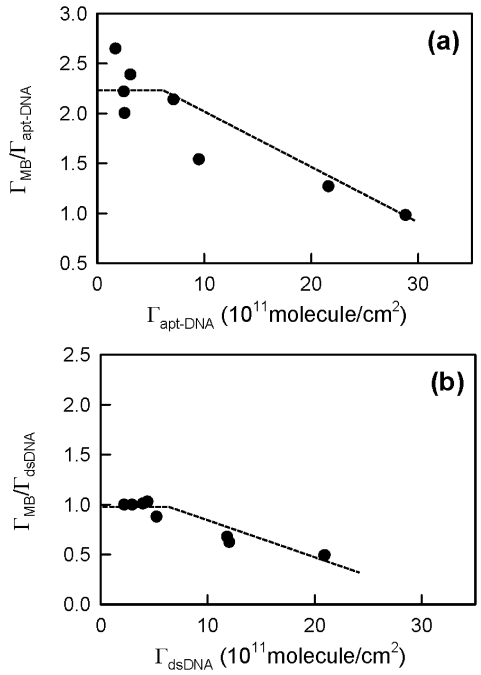

Figure 7. Number of MB molecules bound to (a) apt−DNA and (b) dsDNA as a function of apparent surface density of DNA constructs immobilized on a gold electrode. Each data point was calculated from an on-chip (electrode) CV experiment with 1.0 μM MB without adenosine in binding buffer (electrode area = 0.66 cm^2; scan rate = 100 mV/s). The dashed lines are to guide the eyes only.

it is evident that within the same DNA surface density range the number of MB molecules bound to apt−DNA is always around twice that on dsDNA, indicating that even at higher surface densities of apt−DNA additional MB can stack in the aptamer domain. According to the hypothesis of Kelley et al.,[17] only one MB molecule should intercalate between the terminal GC pairs of both apt−DNA and dsDNA. In fact, as shown in Figure 7, on average 1.0 MB and 0.5 MB are bound to apt−DNA and dsDNA, respectively, when the surface density becomes high (~5×10^{12} molecules/cm^2). Here we have not considered the heterogeneity of the DNA films,[31] which also influences the possibility of MB intercalation in the DNA double helices.

All the above results can be interpreted with the schematic view of the differently bound MB molecules on apt−DNA shown in Figure 8. It is possible that one MB intercalates between the GC pairs located near the solution−electrode interface; one extra MB can reversibly stack with the single guanine base in the aptamer domain of the DNA conformational switch. By introducing or removing the adenosine, this MB can be eliminated into solution or rebind with the aptamer domain.

Adenosine/apt−DNA Binding Isotherm. Compared with gel electrophoresis assay-based biochemical studies,[35] our electrochemical approach is more suitable for investigating the reversibility and selectivity of this DNA conformational switch for binding adenosine. Figure 9 shows that addition of AMP and adenosine resulted in a positive response (decreased

dx.doi.org/10.1021/jp302988t | J. Phys. Chem. B 2012, 116, 6361−6368

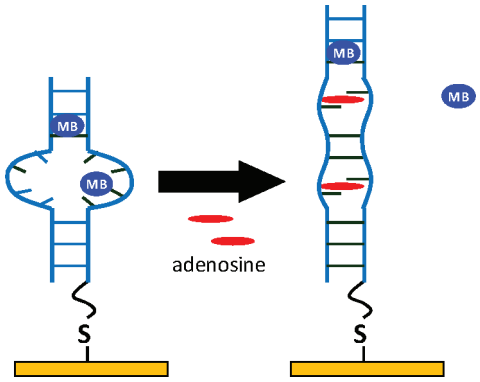

Figure 8. Schematic comparison of the different binding modes of MB to the dsDNA–aptamer construct (apt–DNA) before and after adenosine binding. A MB molecule intercalates in the upper stem of apt–DNA which is not influenced by the adenosine binding. The extra MB stacks on a single guanine in the aptamer domain of apt–DNA are eliminated upon adding adenosine, resulting from the formation of a structurally more compact aptamer–ligand complex.

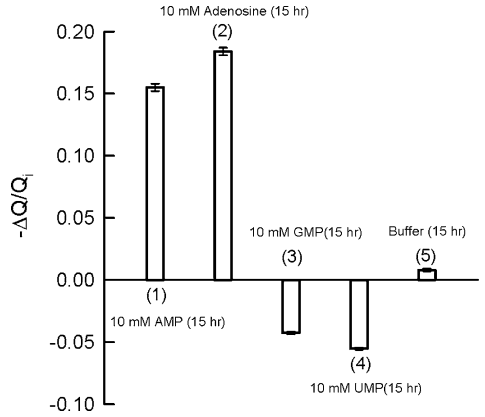

Figure 9. Relative electrochemical signal change for background, positive, and negative controls by adding 1.0 μM MB at an apt–DNA-modified gold electrode: The relative signal decrease normalized over the surface density is plotted above: (1) 15 h incubation with 10 mM AMP; (2) 15 h incubation with 10 mM adenosine; (3) 15 h incubation with 10 mM GMP; (4) 15 h incubation with 10 mM UMP; (5) 15 h incubation with binding buffer. The *y*-axis is the ratio between signal change (ΔQ) and the initial reading (Q_i).

peak current), while GMP and UMP caused relatively, much less significant (but discernible) changes. It has been reported that the same DNA aptamer (Figure 1a) binds ATP, AMP, and adenosine with similar binding affinities.[4] Although the relative binding affinity of adenosine vs AMP to the DNA aptamer was not evaluated previously, the lower signal obtained for AMP may be due to the interaction of the phosphate group with the negatively charged DNA backbone.

The reason for the "negative" signal observed when adding UMP and GMP is not known at this stage, especially the aptamer sequence which was originally selected for binding ATP/adenosine.[4,14] An NMR study by Noeske et al.[46] showed that the aptamers of both guanine and adenosine form intramolecular triplets; the addition of large amounts of GMP may induce the formation of interchain constructs, which in turn increase the number of MB molecules intercalated into the film.

Figure 10(a) shows that the response signal ($-\Delta Q/Q_i$) initially increases with increasing concentration of adenosine in

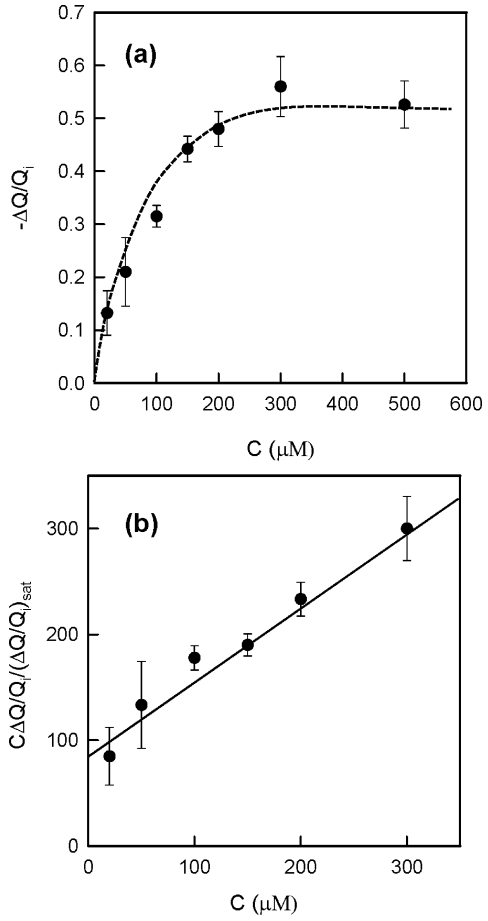

Figure 10. (a) Plot of relative electrochemical signal change as a function of adenosine concentration. Error bars show the variance of data points obtained in three independent CV measurements. The dashed line is to guide the eyes only. (b) A linearized isotherm of adenosine binding to the immobilized dsDNA–aptamer construct. See text for details.

the electrolyte and reaches a plateau above 300 μM. On the basis of the Langmuir model,[38] we further evaluated the dissociation constant of the adenosine/apt–DNA complex on the electrode surface. The classical Langmuir model assumes that every binding site is equivalent and that the ability of a molecule to bind is independent of the occupation of nearby sites. A linearized form of the Langmuir isotherm which correlates the adenosine concentration (C) in solution, the electrochemical signal ($\Delta Q/Q_i$), the saturated signal change $(\Delta Q/Q_i)_{sat}$, and the dissociation constant K_d is given by eq 4

$$\frac{C}{(\Delta Q/Q_i)} = \frac{C}{(\Delta Q/Q_i)_{sat}} + \frac{K_d}{(\Delta Q/Q_i)_{sat}} \quad (4)$$

In Figure 10(b), the value of $C(\Delta Q/Q_i)_{sat}/(\Delta Q/Q_i)$ is plotted as a function of the adenosine concentration (C). From the fitted intercept, we can determine the dissociation constant K_d of the adenosine/apt–DNA complex. The value obtained here (88 ± 10 μM) shows a moderate improvement from that of the strand-displacement design (127 μM)[47] and that from gel electrophoresis experiments (135 μM).[35]

With MB as the model system, we are able to illustrate the "multiplex" modes of binding between "intercalative" small molecules and specially designed dsDNA–aptamer constructs. This will eventually augment the design and construction of the

dx.doi.org/10.1021/jp302988t | J. Phys. Chem. B 2012, 116, 6361–6368

next generation of DNA-based sensing and switching devices with good sensitivity and reproducibility. The reported dissociation constant of adenosine/apt−DNA indicates a moderate binding affinity of the designed dsDNA−aptamer construct for the target ligand on the electrode surface. Several novel strategies to enhance the electrochemical signal in aptamer-based biosensors for adenosine/ATP have been proposed recently,[48−53] e.g., the use of functionalized gold nanoparticles. In conjunction with these novel approaches for signal enhancement, it is entirely possible to develop an ultrasensive adenosine (or other small molecular ligand) sensor based on the design principle of functional dsDNA−aptamer constructs.

CONCLUSION

We have demonstrated that solution-diffused MB can interact with a surface-immobilized dsDNA−aptamer construct in at least two different modes, namely, intercalation and single-base stacking. On the basis of the surface densities of dsDNA and MB determined by cyclic voltammetry, we have shown that one MB molecule can intercalate in a 22-mer dsDNA. Depending upon the surface density of the dsDNA−aptamer construct, at least one extra MB can stack in the aptamer domain, and an adenosine binding-triggered conformational change causes the elimination of this extra MB. The dissociation constant of the adenosine/apt−DNA complex was determined from the binding isotherm, which is a moderate improvement over gel electrophoresis assays and the strand-displacement design. Our investigations of further analytical aspects of the functional dsDNA−aptamer construct are currently underway.

ASSOCIATED CONTENT

Supporting Information

Experimental results of electrochemistry of $K_3Fe(CN)_6$ and MB with a bare and an apt−DNA-modified gold electrode and Laviron plots of MB intercalating apt−DNA. This material is available free of charge via the Internet at http://pubs.acs.org.

AUTHOR INFORMATION

Corresponding Author

*E-mail: hogan_yu@sfu.ca.

Notes

The authors declare no competing financial interest.

ACKNOWLEDGMENTS

This research was supported by the Natural Science and Engineering Research Council of Canada (NSERC). We wish to thank Dr. Dipankar Sen for useful discussions and suggestions, and Dr. Eberhard Kiehlmann for editing the manuscript.

REFERENCES

(1) Tuerk, C.; Gold, L. *Science* **1990**, *249*, 505−510.
(2) Ellington, A. D.; Szostak, J. W. *Nature* **1990**, *346*, 818−822.
(3) Hornung, V.; Limmer, S.; Hofmann, H. P. *RNA* **1997**, *3*, 1289−1300.
(4) Huizenga, D.; Szostak, J. W. *Biochemistry* **1995**, *34*, 656−665.
(5) Bock, L. C.; Griffin, L. C.; Latham, J. A.; Vermaas, E. H.; Toole, J. J. *Nature* **1995**, *335*, 546−566.
(6) Iliuk, A. B.; Hu, L.; Tao, W. A. *Anal. Chem.* **2011**, *83*, 4440−4453.
(7) Yamamoto, R.; Baba, T.; Kumar, P. K. *Genes Cells* **2000**, *5*, 389−396.
(8) Nutiu, R.; Li, Y. *J. Am. Chem. Soc.* **2003**, *125*, 4771−4778.
(9) Wei, H.; Li, B.; Li, J.; Wang, E.; Dong, S. *Chem. Commun.* **2007**, 3735−3737.
(10) Liu, J.; Lu, Y. *Nat. Protoc.* **2006**, *1*, 246−252.
(11) Tombelli, M.; Minunni, M.; Luzi, E.; Mascini, M. *Bioelectrochemistry* **2005**, *67*, 135−141.
(12) Corn, R. M.; Lee, H. J.; Li, Y. *Anal. Chem.* **2007**, *79*, 1082−1088.
(13) Gronewold, T. M.; Glass, S.; Quandt, E.; Famulok, E. *Biosens. Bioelectron.* **2005**, *20*, 2044−2052.
(14) Lin, H. C.; Patel, J. D. *Chem. Biol.* **1997**, *4*, 817−832.
(15) Song, S.; Wang, L.; Li, J.; Zhao, J.; Fan, C. *Trends Anal. Chem.* **2008**, *27*, 108−117.
(16) Cheng, A. K. H.; Sen, D.; Yu, H.-Z. *Bioelectrochem.* **2009**, *77*, 1−12.
(17) Kelley, S. O.; Barton, J. K.; Jackson, N. M.; Hill, M. G. *Bioconjugate Chem.* **1997**, *8*, 31−37.
(18) Ju, H.; Zhou, J.; Cai, C.; Chen, H. *Electroanalysis* **1995**, *7*, 1165−1170.
(19) Xiao, Y.; Lubin, A. A.; Heeger, A. J.; Plaxco, K. W. *Angew. Chem., Int. Ed.* **2005**, *44*, 5456−5459.
(20) Tani, A.; Thomson, A. J.; Butt, J. N. *Analyst* **2001**, *126*, 1756−1759.
(21) Castano-Alvarez, M.; Fernandez-la-Villa, A.; Fernandez-Abedul, M. T.; Costa-Garcia, A. *Electrophoresis* **2007**, *28*, 4679−4689.
(22) Rohs, R.; Sklenar, H.; Lavery, R.; Roder, R. *J. Am. Chem. Soc.* **2000**, *122*, 2860−2866.
(23) Tuite, E.; Norden, B. *J. Am. Chem. Soc.* **1994**, *116*, 7548−7556.
(24) Laustrait, G. *Biochemie* **1986**, *68*, 771−778.
(25) Muller, W.; Crothers, D. M. *Eur. J. Biochem.* **1975**, *54*, 267−277.
(26) Ohuigin, C; McConnell, D. J.; Kelly, J. M.; Van der Putten, V. J. M. *Nucleic Acids Res.* **1987**, *45*, 167−75.
(27) Tong, C.; Zhou, H.; Wu, J. *J. Fluoresc.* **2010**, *20*, 261−267.
(28) Yang, W.; Ozsoz, M.; Hibbert, B. D.; Gooding, J. J. *Electroanalysis* **2002**, *18*, 1299−1302.
(29) Gheorghe, V.; Levy, B.; Enescu, M. *J. Phys. Chem. B* **2000**, *104*, 1073−1077.
(30) Bang, G. S.; Cho, S.; Kim, B. G. *Biosens. Bioelectron.* **2005**, *21*, 863−870.
(31) Wang, J. L.; Wang, F. A.; Dong, S. J. *J. Electroanal. Chem.* **2009**, *626*, 1−5.
(32) Jin, Y.; Yao, X.; Liu, Q.; Li., J. *Biosens. Bioelectron.* **2007**, *22*, 1126−1130.
(33) Zhu, L.; Zhao, R.; Wang, K.; Xiang, H.; Shang, Z.; Sun, W. *Sensors* **2008**, *80*, 8028−8034.
(34) Kerman, K.; Ozkan, D.; Kara, P.; Meric, B.; Gooding, J. J.; Ozsoz, M. M. *Anal. Chim. Acta* **2002**, *462*, 38−47.
(35) Fahlman, R. P.; Sen, D. *J. Am. Chem. Soc.* **2002**, *124*, 4610−4616.
(36) Yu, H.-Z.; Luo, C.-Y.; Sankar, C. G.; Sen, D. *Anal. Chem.* **2003**, *75*, 3902−3907.
(37) Ge, B.; Huang, Y. C.; Sen, D.; Yu, H.-Z. *J. Electroanal. Chem.* **2007**, *602*, 156−162.
(38) Su, L.; Sankar, C. G.; Sen, D.; Yu, H.-Z. *Anal. Chem.* **2004**, *76*, 5953−5959.
(39) Simonsson, T. *Biol. Chem.* **2001**, *382*, 621−628.
(40) Boon, E. M.; Jackson, N. M.; Wightman, M. D.; Kelley, S. O.; Hill, M. G.; Barton, J. K. *J. Phys. Chem. B* **2003**, *107*, 11805−11812.
(41) Slinker, J. D.; Muren, N. B.; Renfrew, S. E.; Barton, J. K. *Nat. Chem.* **2011**, *3*, 228−233.
(42) Laviron, E. *J. Electroanal. Chem.* **1979**, *101*, 19−28.
(43) Zutic, V.; Svetlicic, V.; Lovric, M.; Ruzic, I.; Chevalet, J. *J. Electroanal. Chem.* **1984**, *177*, 253−268.
(44) Herman, T.; Patel, J. D. *Science* **2000**, *287*, 820−825.
(45) Crothers, D. M. *Biopolymers* **1968**, *6*, 575−584.
(46) Noeske, J.; Richter, C.; Grundl, M. A.; Nasiri, H. R.; Schwalbe, H.; Wohnert, J. *Proc. Natl. Acad. Sci. U.S.A.* **2005**, *102*, 1372−1377.
(47) Chakraborty, B.; Jiang, Z.; Li, Y.; Yu, H.-Z. *J. Electroanal. Chem.* **2009**, *635*, 75−82.
(48) Monstserrat, J. M.; Ramirez, S. A.; Ponce, B.; Ceretti, H. *Electroanlysis* **2009**, *22*, 147−150.

(49) Zayats, M.; Huang, Y.; Gill, R.; Ma, C. A.; Willner, I. *J. Am. Chem. Soc.* **2006**, *128*, 13666−13667.
(50) Zhang, S.; Xia, J.; Li, X. *Anal. Chem.* **2008**, *80*, 8382−8388.
(51) Liu, Z.; Yuan, R.; Chai, Y.; Zhuo, Y.; Hong, C.; Yang, X.; Su, H.; Qian, X. *Electrochim. Acta* **2009**, *54*, 6207−6211.
(52) Feng, K.; Sun, C.; Kang, Y.; Chen, J.; Jiang, J.; Shen, G.; Yu, R. Q. *Electrochem. Commun.* **2008**, *10*, 531−535.
(53) Zuo, X.; Song, S.; Zhang, J.; Pan, D.; Wang, L.; Fan, C. *J. Am. Chem. Soc.* **2007**, *129*, 1042−1043.